

Oxygen at High Pressures : Theoretical Approach to Monoatomic Phases

メタデータ	言語: eng 出版者: 公開日: 2017-10-03 キーワード (Ja): キーワード (En): 作成者: メールアドレス: 所属:
URL	https://doi.org/10.24517/00011075

This work is licensed under a Creative Commons Attribution-NonCommercial-ShareAlike 3.0 International License.



Oxygen at high pressures : theoretical approach to monoatomic phases

T. Oda¹, K. Sugimori¹, H. Nagao¹, I. Hamada², S. Kagayama³,
M. Geshi³, H. Nagara³, K. Kusakabe³, and N. Suzuki³

¹Graduate School of Natural Science and Technology, Kanazawa University,
Kanazawa 920-1192, Japan

² Department of Condensed Matter Physics, The Institute of Scientific and Industrial
Research(ISIR), Osaka University, 8-1 Mihogaoka, Ibaraki, Osaka 567-0047, Japan

³ Division of Material Physics, Department of Physical Science, Graduate School of
Engineering Science, Osaka University, Toyonaka 560-8531, Japan

E-mail: oda@cphys.s.kanazawa-u.ac.jp

Abstract. We have studied the ζ -phase of solid oxygen with using the generalized gradient approximation in the density functional approach. The free energy calculation has been carried out for the prototype of diatomic ζ -phase and other hypothetical monoatomic crystal structures. The diatomic phase was found to be stable in a wide range of pressure (100-2000 GPa). The stacking of molecular layers was discussed in comparison with the available experimental data.

1. Introduction

Oxygen consists of diatomic magnetic molecule, which has a spin-triplet ground state under low pressures. This molecular magnetism is the main origin of paramagnetic or antiferromagnetic properties of condensed oxygens. In the ε -phase, the quench of magnetic long range order was reported in the spin-polarized neutron diffraction measurement [1]. Recently, the unique crystal structure of oxygen, $(\text{O}_2)_4$ molecular lattice, has been determined at the ε -phase by Fujihisa *et al.*. Their Rietveld analysis for the x-ray diffraction measurements in powder samples shows a much better fit, compared with that of the previous structure model [2]. Successively, results of the $(\text{O}_2)_4$ lattice were reported for single crystal samples [3]. This molecular picture at the low pressures in ε -phase gradually changes, as pressure increases, to the two-dimensional one which consists of aligned molecules. The structural phase transition to the ζ -phase has been observed at 96 GPa [4].

High pressures on oxygen have induced the appearance of metallic feature. Even the superconducting property was also reported around 100 GPa in ζ -phase [5]. Above the transition pressure, the existence of molecular vibrations have been indicated in the Raman measurement [6]. Serra *et al.* found a prototype for the ζ -phase in the simulation which starts from the structure of δ -phase. At the phase transition, the sliding of

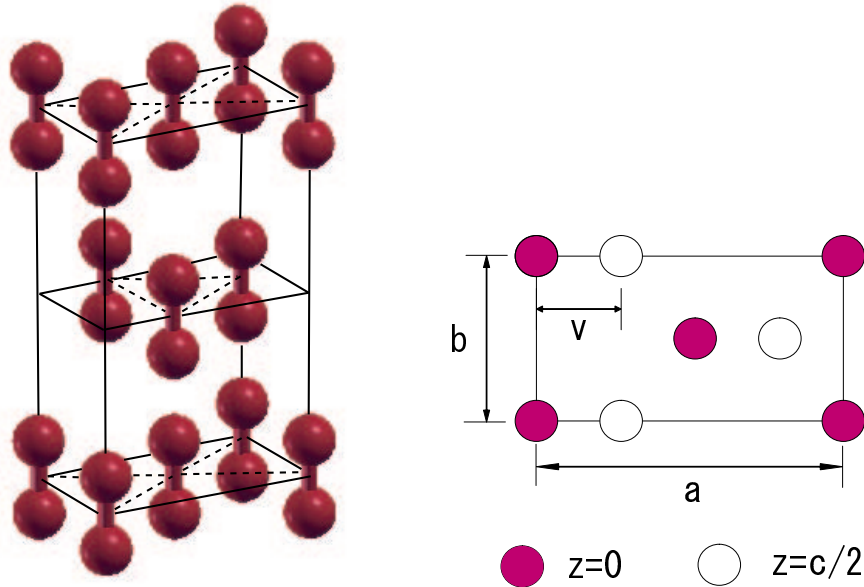


Figure 1. The prototype crystal structure for ζ -phase, found by Serra *et al.* [7].

molecular layer has been discussed in the previous works [6, 7]. The structure proposed by Serra *et al.* is consistent with keeping a molecular form. The first experiment of x-ray measurement for powder samples reported six diffraction peaks at 116 GPa. For single crystal samples, Weck *et al.* captured at 110 GPa the four diffraction angles [6]. These angles contain the diffraction which have shown only slight change and keeps the same angles. The two of four angles have been discussed in relation with the sliding of molecular layers.

As pressure increases to a high value, monoatomic phases would be expected, as observed in I_2 , Br_2 , Cl_2 [8, 9, 10, 11]. Otani *et al.* studied on the monoatomic phases by using a linearized muffin-tin orbital method and discussed the stability of β -Po structure, compared with bcc structure [12]. Neaton *et al.* provided the free energy curve of ζ -phase at the pressures lower than 80 GPa [13].

To find a monoatomic phase of solid oxygen, we have studied the structural properties and the stability of typical monoatomic and molecular phases in oxygen. We have calculated the free energy of crystal structures at zero temperature as a function of pressure. The diatomic ζ -phase is found to be stable in a wide range of pressure.

2. Method and crystal structures

For the density functional theory(DFT) [14], we used planewave basis to represent wavefunctions and electron densities and ultrasoft-type pseudopotentials [15, 16] to include core-valence interactions. The $1s$ states were included in the core, while the other states were described explicitly. In the construction of pseudopotentials, we took the cut-off radius of 0.609 \AA with including a d -symmetry local orbitals [17]. The energy cut-offs of 100 and 400 Ry were taken for wavefunction and electron density, respectively. The

exchange and correlation energy was treated in the generalized gradient approximation proposed by Perdew and Wang (PW91) [18]. We used the sets of special points for sampling \mathbf{k} points [19]. The ground state of molecule corresponds to the spin-polarized state with a magnetization of $2 \mu_B$ and shows a bond length of 1.22 Å, a vibrational frequency of 46.7 THz, and a binding energy of 5.99 eV. The two former are in good agreement with the corresponding experimental values (1.21 Å, 47.39 THz) and the latter is larger than the experimental value (5.12 eV) by 17 % [20]. These properties are similar to the previous results in density functional approaches to oxygen [7, 13, 17].

The crystal structure of ζ -phase has not been determined experimentally, but, since Serra *et al.* proposed an base-centered orthorhombic structure, presented by the space group of $C2mm$, it has been used for a prototype of ζ -phase [13, 21]. Figure 1 present the crystal structure and we call it the prototype in this paper. The parameters of the structure are a, b, c, v, f . The last parameter of f specifies the bond length of molecule. This prototype also implies that the aligned molecules form a triangular lattice in the ab -plane. This property is presented by the ratio of $b/a \sim 1/\sqrt{3}$. The prototype has a hexagonal-closed-packed layer stacking for the c -direction. We also treated it a hexagonal lattice in our work. We also considered a cubic-closed-packed layer stacking for c -direction. This structure can be treated as a rhombohedral lattice.

For monoatomic crystal structures, we considered the β -Po structure, as in the previous work [12]. It is convenient to investigate this structure because it contains typical simple structures (fcc, sc, bcc) in variations of lattice parameters. We also considered the hexagonal closed packing (hcp) and simple hexagonal (sh) structures. Because these structures have much larger energy than the optimized structures in β -Po structure, we do not present results in this paper.

In this work, we optimize the structural parameters by using calculated pressures and atomic forces. For a given pressure, the free energy (enthalpy) is estimated with total energy (E), the pressure (p) and the volume (Ω); $G = E + p\Omega$. For the sampling \mathbf{k} points, we used the $12 \times 12 \times 10$ mesh for the prototype of ζ -phase, and the $16 \times 16 \times 16$ for the β -Po structure of monoatomic phase. When we need an accuracy to free energies, we used the $26 \times 26 \times 26$ mesh for the trigonal system of one-molecule unit cell and the $18 \times 18 \times 18$ mesh for the hexagonal system of two-molecule unit cell. The above convergence amounts to 0.2 meV/atom in the trigonal and 1.4 meV/atom in the hexagonal at 1920 GPa. At the lower pressures, the accuracy would become to higher.

3. Results and discussions

The monoatomic phase of β -Po structure has two lattice parameters. Figure 2 presents total energies for various parameters, volume (Ω) and cosine of trigonal angle ($\cos \alpha_r$). At the larger volumes (low pressures), simple cubic (sc) structures, having $\cos \alpha_r = 0$, has the lowest energy. At the smaller volumes, the lowest energy state changes to the β -Po structure which has $\cos \alpha_r$ of $-0.20 \sim -0.25$ (β -Po-I). The body centered cubic (bcc) does not take a lowest energy state for the volume range of $2.50 \sim 6.40 \text{ \AA}^3/\text{atom}$.

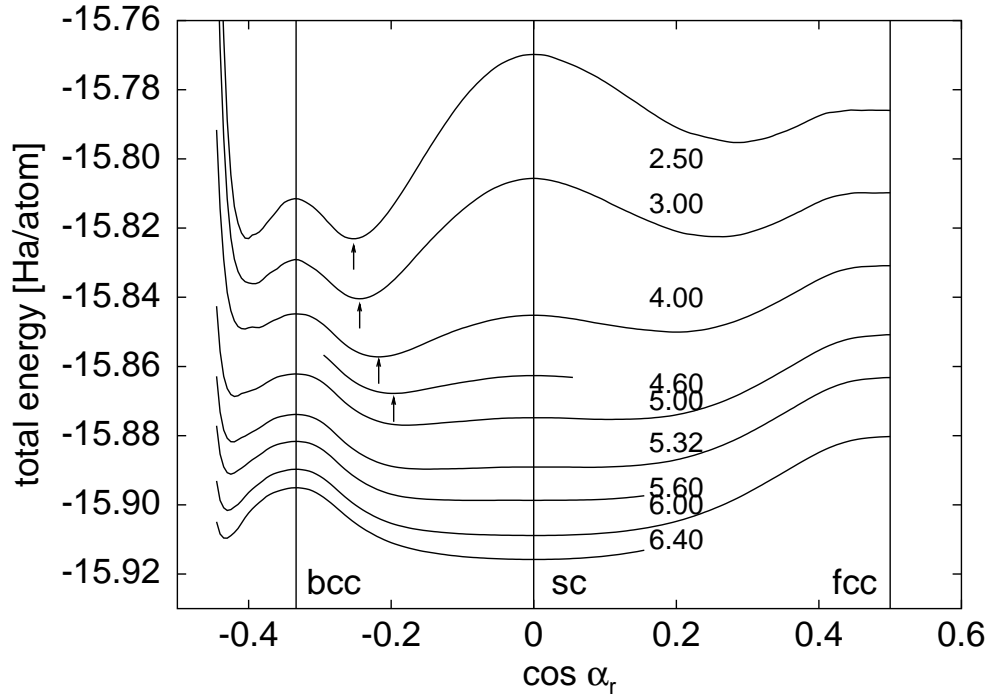


Figure 2. Total energy E of β -Po structures as a function of lattice parameter, $\cos \alpha_r$, where α_r is the angle between the couple of trigonal axes. The curve specifies a variation for a fixed volume and the curves are shifted to downward to draw them in the same figure; shifted by 0.012, 0.050, 0.200, 0.350 Ha for $\Omega = 4.60, 4.00, 3.00, 2.50 \text{ \AA}^3/\text{atom}$. The arrows point at the minima of E_f or a given volume.

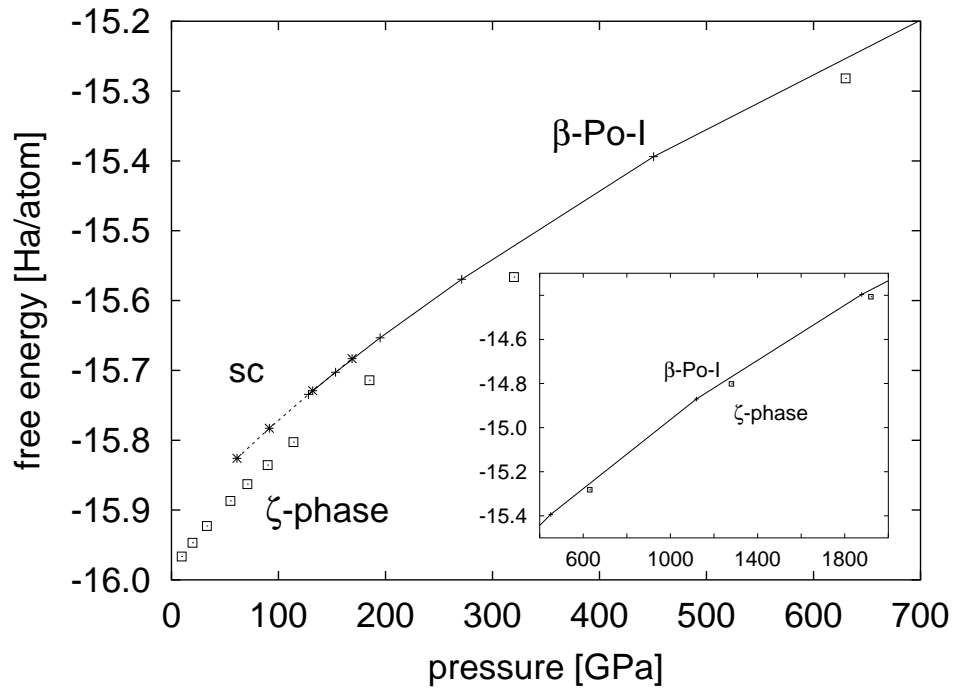


Figure 3. Enthalpy as a function of pressure in the oxygen of high-pressure structures; β -Po structure(plus), simple cubic structure(star) and the prototype of ζ -phase(box).

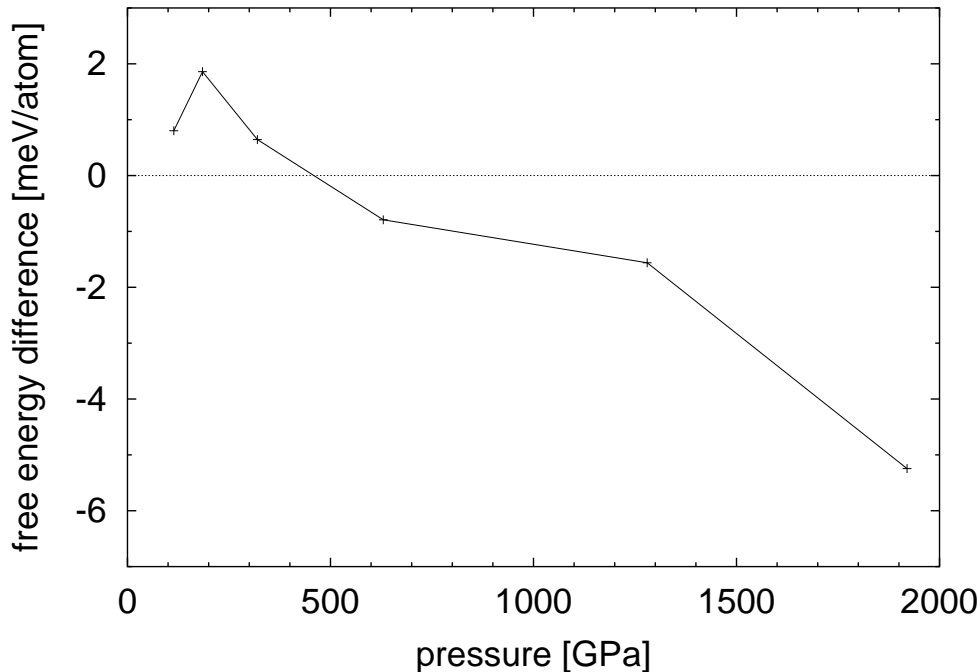


Figure 4. The free energy (enthalpy) of the diatomic trigonal structure with respect to that of the diatomic hexagonal structure.

The semi-stable state appears at the parameters of $\cos \alpha_r$ of $-0.40 \sim -0.43$ (β -Po-II). Our result described above is a similar one to the previous work [12], corresponding to a more qualified version in the β -Po structure. In our work, pressures are also calculated and the results are compared with the prototype of diatomic phases in free energy, as presented later.

The prototype structure of ζ -phase was found to be stable in the wide range of pressure. In Fig. 3, the free energy as a function of pressure is presented for the prototype of ζ -phase, compared with sc and β -Po-I, at the pressures up to 2000 GPa. The prototype of ζ -phase is much lower in free energy than the β -Po-I of monoatomic phase. The bond length of molecules (1.180 Å at 114 GPa) is gradually decreased to 1.034 Å at 1920 GPa. The atomic distances between molecular layers are 2.193, 1.589 Å for 114 and 1920 GPa, respectively. These are still far from intramolecular bond lengths. The stability of the prototype might be attributed to a closed packing of molecules in the ab -plane, as well as a formation of molecular bond. Indeed, the structure parameters obtained for the prototype show that $b/a \sim 0.57$ and $v/a \sim 0.33$ at the all pressures we investigated.

We also calculated the free energy of two molecule unit cell with the hexagonal constraint, obtaining a similar free energy to the structure of $C2mm$. We considered another structure with an ABC stacking along c -direction (the trigonal structure), while the prototype has an AB stacking. The molecular layer of O_2 in the ab -planes would be rigid and it is interesting to compare energies for the sequence of stacking, to access the

Table 1. The reciprocal lattice vectors whose diffractions provide relatively large peaks in the hexagonal and trigonal structures. The a_{hex} and d_0 ($\equiv c_{\text{hex}}/2$) are the lattice parameter of triangular lattice and the distance of molecular layers, respectively. The opposite directions of the listed vectors should be added to obtain the full representation.

hexagonal	trigonal
$\vec{G}_{\text{h}0}(002) = \frac{2\pi}{d_0} \vec{e}_z$	$\vec{G}_{\text{t}0}(111) = \frac{2\pi}{d_0} \vec{e}_z$
$\vec{G}_{\text{h}1}(010) = \frac{2\sqrt{3}}{3} \frac{2\pi}{a_{\text{hex}}} \vec{e}_y$	$\vec{G}_{\text{t}1}(100) = \frac{2\pi}{a_{\text{hex}}} \vec{e}_x + \frac{\sqrt{3}}{3} \frac{2\pi}{a_{\text{hex}}} \vec{e}_y + \frac{2}{3} \frac{2\pi}{2d_0} \vec{e}_z$
$\vec{G}_{\text{h}1}(1\bar{1}0) = \frac{2\pi}{a_{\text{hex}}} \vec{e}_x - \frac{\sqrt{3}}{3} \frac{2\pi}{a_{\text{hex}}} \vec{e}_y$	$\vec{G}_{\text{t}1}(010) = -\frac{2\pi}{a_{\text{hex}}} \vec{e}_x + \frac{\sqrt{3}}{3} \frac{2\pi}{a_{\text{hex}}} \vec{e}_y + \frac{2}{3} \frac{2\pi}{2d_0} \vec{e}_z$
$\vec{G}_{\text{h}1}(010) = \frac{2\pi}{a_{\text{hex}}} \vec{e}_x + \frac{\sqrt{3}}{3} \frac{2\pi}{a_{\text{hex}}} \vec{e}_y$	$\vec{G}_{\text{t}1}(001) = -\frac{2\sqrt{3}}{3} \frac{2\pi}{a_{\text{hex}}} \vec{e}_y + \frac{2}{3} \frac{2\pi}{2d_0} \vec{e}_z$
$\vec{G}_{\text{h}2}(011) = \frac{2\sqrt{3}}{3} \frac{2\pi}{a_{\text{hex}}} \vec{e}_y + \frac{2\pi}{2d_0} \vec{e}_z$	$\vec{G}_{\text{t}2}(011) = -\frac{2\pi}{a_{\text{hex}}} \vec{e}_x - \frac{\sqrt{3}}{3} \frac{2\pi}{a_{\text{hex}}} \vec{e}_y + \frac{4}{3} \frac{2\pi}{2d_0} \vec{e}_z$
$\vec{G}_{\text{h}2}(01\bar{1}) = \frac{2\sqrt{3}}{3} \frac{2\pi}{a_{\text{hex}}} \vec{e}_y - \frac{2\pi}{2d_0} \vec{e}_z$	$\vec{G}_{\text{t}2}(101) = \frac{2\pi}{a_{\text{hex}}} \vec{e}_x - \frac{\sqrt{3}}{3} \frac{2\pi}{a_{\text{hex}}} \vec{e}_y + \frac{4}{3} \frac{2\pi}{2d_0} \vec{e}_z$
$\vec{G}_{\text{h}2}(1\bar{1}\bar{1}) = \frac{2\pi}{a_{\text{hex}}} \vec{e}_x - \frac{\sqrt{3}}{3} \frac{2\pi}{a_{\text{hex}}} \vec{e}_y + \frac{2\pi}{2d_0} \vec{e}_z$	$\vec{G}_{\text{t}2}(110) = \frac{2\sqrt{3}}{3} \frac{2\pi}{a_{\text{hex}}} \vec{e}_y + \frac{4}{3} \frac{2\pi}{2d_0} \vec{e}_z$
$\vec{G}_{\text{h}2}(1\bar{1}\bar{1}) = \frac{2\pi}{a_{\text{hex}}} \vec{e}_x - \frac{\sqrt{3}}{3} \frac{2\pi}{a_{\text{hex}}} \vec{e}_y - \frac{2\pi}{2d_0} \vec{e}_z$	
$\vec{G}_{\text{h}2}(101) = \frac{2\pi}{a_{\text{hex}}} \vec{e}_x + \frac{\sqrt{3}}{3} \frac{2\pi}{a_{\text{hex}}} \vec{e}_y + \frac{2\pi}{2d_0} \vec{e}_z$	
$\vec{G}_{\text{h}2}(10\bar{1}) = \frac{2\pi}{a_{\text{hex}}} \vec{e}_x + \frac{\sqrt{3}}{3} \frac{2\pi}{a_{\text{hex}}} \vec{e}_y - \frac{2\pi}{2d_0} \vec{e}_z$	

structure of ζ -phase. The sliding of layers inferred at the phase-transition from ε -phase to ζ -phase encourages an investigation of stacking for molecular layers. In Fig. 4 the energy differences are presented. At the high pressures, the free energy of the trigonal structure is slightly lower than that of the hexagonal one. However, the differences are only a few factor of the accuracy of \mathbf{k} -point sampling.

The stacking of molecular layers causes the diffraction peaks which correspond the spacings of the layers. In the calculated structures at 114 GPa, the spacings of the layers (d_0) are 3.009 and 3.010 Å for hexagonal and trigonal structures, respectively, which compare to the values (2.9858 Å [6], 2.9852 Å [4]) from the experiments. The calculated values are larger by 0.8 % than the experimental ones, which shows a typical accuracy of the DFT approach. The lattice constant in ab -planes (a_{hex}) is estimated to be 2098 and 2.099 Å at 114 GPa.

The some of diffraction angles in the trigonal structure coincide with the observed diffraction angles in the ζ -phase. For the hexagonal and trigonal structures, the diffraction angles are calculated with using the formula of the reciprocal lattice vectors which are given in Table 1. In this table, the reciprocal lattice vectors which are expected to provide larger peaks in x-ray diffraction measurements are listed only. The diffraction angles are summarized in Table 2, compared with the result of the x-ray diffraction measurement for single crystal samples [6]. The pairs of $\vec{G}_{\text{t}1}$ and $\vec{G}_{\text{t}2}$, for example, forms the couple of angles. As seen in Table 2, the three experimental values would correspond to the angles from the trigonal structure. The fact that the diffraction peaks from $\vec{G}_{\text{t}1}$ and $\vec{G}_{\text{t}2}$ are identified as the diffractions which have been related with

Table 2. The angles (in degree) between the diffraction planes at 114 GPa. $\theta_{s,s'}$ specifies the angle between the reciprocal lattice vectors, \vec{G}_s and $\vec{G}_{s'}$. The experimental data in parentheses are compiled from the table 1 in ref. [6]. At the last row, the angles are listed, assuming the lattice parameters ($a_{\text{hex}} = 2.1297 \text{ \AA}$, $d_0 = 2.9858 \text{ \AA}$).

	θ_{h_0,h_1}	θ_{h_0,h_2}	θ_{h_1,h_2}	θ_{t_0,t_1}	θ_{t_0,t_2}	θ_{t_1,t_2}	others
cal.	90	73.2	16.8, 56.4	78.6	68.1	33.3, 58.1	
(exp.)				(78.5)	(67.2)	(34.3)	(60.7)(61.5)(77.7)
parameter	90	72.8	17.2, 56.5	78.4	67.6	34.0, 58.0	

Table 3. The d spacings (in \AA) of the diffraction planes for the trigonal structure at 114 GPa, compared with the experimental data at 116 and 110 GPa [4, 6].

	d_{t_0}	d_{t_1}	d_{t_2}	d_{u_1}	d_{u_2}
cal.	3.01	1.78	1.69		
Weck <i>et al.</i>	2.9858	1.7819	1.6946		1.8444
Akahama <i>et al.</i>	2.9852	1.7782	1.7119	1.9752	1.8601

the sliding of molecular layers at the phase transition in the experiment [6], largely supports an appearance of ABC stacking of layers instead of a hexagonal(AB) one in the ζ -phase.

For the trigonal structure, the d spacings of diffraction planes are listed in Table 3, compared with the experimental values. The calculated d spacings agree with the experimental values, while the couple of d spacings in experiments remains unresolved, which are called d_{u_1} and d_{u_2} in this work. The diffraction of d_{u_2} have been observed in both powder and single crystal samples. The value of d_{u_2} is similar to the value of d_{h_1} . At the last row in Table 2, we list the angles when we assume $a_{\text{hex}} = 2.1297 \text{ \AA}$ ($= 2\sqrt{3}d_{u_2}/3$) and $d_0 = 2.9858 \text{ \AA}$. The series of trigonal is consistent with the experimental data. However the diffraction angle from the $\vec{G}_{t_0}(111)$ (normal to the molecular plane) is estimated to be 60.7 degree in experiment, being inconsistent with $\theta_{h_1,t_0} = 90$ degree.

The ABC stacking of molecular layers may explain a part of structural properties in ζ -phase. However, a satisfied understanding to the structure is very far. The diffractions of d_{u_1} and d_{u_2} have not shown any drastic change at the phase transition unlike the d_{t_1} and d_{t_2} . The one of θ_{t_1,t_2} has never been observed yet. The intraplanar atomic position would be determined to solve the crystal structure in the high pressure phase.

4. Summary

We have investigated the high pressure phases in the range between 100 and 2000 GPa. The monoatomic phases, which have β -Po structures, are not lower in energy than the prototype of diatomic ζ -phase. This implies a stability of diatomic structures in

a wide range of pressure. The free energy calculations for the *ABC* and *AB* stacking of molecular layers show that the former is slightly more stable than the latter at high pressures. It was found from the angle analysis between diffraction planes that the *ABC* stacking was more favorable than the *AB* stacking, compared with the available experimental data.

Acknowledgments

The calculation in this work was carried out using the facilities of the Supercomputer Center, Institute for Solid State Physics, University of Tokyo. The authors have been partially supported by a Grant-in-Aid for Scientific Research in Priority Areas, Development of New Quantum Simulators and Quantum Design (Nos. 17064009 and 17064013), of The Ministry of Education, Culture, Sports, Science, and Technology, Japan. One of the authors (T.O.) would like to thank the Japan Society for the Promotion of Science for financial support (No. 17510097).

References

- [1] Goncharenko I N 2005 *Phys. Rev. Lett.* **94** 205701
- [2] Fujihisa H, Akahama Y, Kawamura H, Ohishi Y, Shimomura O, Yamawaki H, Sakashita M, Gotoh Y, Takeya S and Honda K 2006 *Phys. Rev. Lett.* **97** 085503
- [3] Lundegaard L F, Weck G, McMahon M I, Desgreniers S, Loubeyre P 2006 *Nature (London)* **443** 201
- [4] Akahama Y, Kawamura H, Häusermann D, Hanfland M, and Shimomura O 1995 *Phys. Rev. Lett.* **74** 4690
- [5] Shimizu K, Suhara K, Ikumo M, Eremets M I and Amaya K 1998 *Nature (London)* **393** 767
- [6] Weck G, Loubeyre P, and LeToullec R 2002 *Phys. Rev. Lett.* **88** 035504
- [7] Serra S, Chiarotti G, Scandolo S, and Tosatti E, 1998 *Phys. Rev. Lett.* **80** 5160
- [8] Takemura K, Minomra S, Shimomura O and Fuji Y 1980 *Phys.Rev.Lett.* **45** 1881
- [9] Takemura K, Sato K, Fujihisa H and Onoda M 2003 *Nature* **423** 971
- [10] Fujii Y, Hase K, Ohishi Y, Fujihisa H, and Hamaya N, 1989 *Phys.Rev.Lett.* **63** 536
- [11] Fujihisa H, Fujii Y, Takemura K and Shimomura O 1995 *J. Phys. Chem. Solids* **56** 1439
- [12] Otani M, Yamaguchi K, Miyagi H and Suzuki N 1998 *Rev. High Pressure Sci. Technol.* **7** 178
- [13] Neaton J B and Ashcroft N W 2002 *Phys. Rev. Lett.* **88** 205503
- [14] Hohenberg H and Kohn W 1964 *Phys. Rev.* **136** B864 ; Kohn W and Sham L J 1965 *Phys. Rev.* **140** A1133
- [15] Vanderbilt D 1990 *Phys. Rev. B* **41** 7892
- [16] Pasquarello A, Laasonen K, Car R, Lee C and Vanderbilt D 1992 *Phys. Rev. Lett.* **69** 1982; Laasonen K, Pasquarello A, Car R, Lee C and Vanderbilt D 1993 *Phys. Rev. B* **47** 10142
- [17] Militzer B, Gygi F, and Galli G 2003 *Phys. Rev. Lett.* **91** 265503
- [18] Perdew J P, Chevary J A, Vosko S H, Jackson K A, Pederson M R, Singh D J and Fiolhais C 1992 *Phys. Rev. B* **46** 6671
- [19] Monkhost H J and Pack J D 1976 *Phys. Rev. B* **13** 5188
- [20] Huber K P and Herzberg G 1979 *Molecular Spectra and Molecular Structure: IV. Constants of Diatomic Molecules* (Van Nostrand Reinhold Company, New York) p. 490
- [21] Otani M, Yamaguchi K, Miyagi H and Suzuki N 1998 *J. Phys.: Condens. Matter* **10** 11603